Laser-noise-induced polarization fluctuations as a spectroscopic tool

R. Walser
Institut für theoretische Physik, Universität Innsbruck, A-6020 Innsbruck, Austria

P. Zoller
Joint Institute for Laboratory Astrophysics, University of Colorado, Boulder, Colorado 80309-0440
(Received 23 November 1993)

We have investigated theoretically the possibility of employing noisy laser fields for spectroscopic purposes. The basis for this spectroscopy is a modification of the statistic of the fluctuations caused by the nonlinear interaction. All atomic resonances within the range of several bandwidths can be observed in the power spectrum, even in case of large inhomogeneous broadening. We have derived analytical, nonperturbative results for a real Gaussian, a complex Gaussian, and a phase-diffusing field. The mean transmitted intensity and its variance as well as the power spectrum have been evaluated in the limit of weak absorption for two-level systems. Without modification, we can apply our results also to other transition schemes. As an example, the power spectrum of the D_2 transition of ^{133}Cs driven by a phase-diffusing field is calculated. For this four-level system we find qualitative agreement with experimental results by Yabuzaki *et al.* [Phys. Rev. Lett. **67**, 2453 (1991)].

PACS number(s): 42.62.Fi, 42.25.Ja, 42.25.Bs, 42.50.Hz

I. INTRODUCTION

Most of the theoretical and experimental work on nonlinear atomic dynamics in stochastic (noisy) laser fields has concentrated on describing the mean response of the atom to the incident light field. For low light intensities and a one-photon transition the atomic response is characterized by the spectrum of the light (the first-order correlation function). For high intensities (saturation) and multiphoton transitions the atomic dynamics depends on the higher-order statistics of the light field as described by the higher-order correlation functions. Recent studies have investigated variances and spectra of atomic fluctuations. In particular, population fluctuations in two-level atoms—as seen in the intensity fluctuations of light emitted in resonance fluorescence from an atomic sample—were shown to be a very sensitive probe of the higher-order statistics of the light, thus providing a new tool in terms of a "noise spectroscopy of atoms" [1–5] (for corresponding experiments see Refs. [6, 7]).

In the present paper we will present a theoretical study of (the change of) intensity fluctuations and corresponding intensity spectra of laser light induced by propagation in a weakly absorbing medium. We will show that these intensity fluctuations are related to *polarization fluctuations* in the atomic medium. Yabuzaki *et al.* [8] have recently observed intensity noise spectra in absorption spectra of alkali-metal-atom vapor with diode lasers. They have shown that the excess intensity noise contains information about the interacting atoms. In particular, they have measured the intensity power spectrum when the laser was tuned near the D_2 transition of ^{133}Cs and observed all corresponding hyperfine-splitting resonances.

A related, more recent experiment has been performed by McIntyre *et al.* [9]. They report intensity noise spectra of a broad-bandwidth laser beam which had passed through a rubidium vapor cell. In comparing it with a theoretical model based on the characteristics of a weakly saturating phase-diffusing field they also found good agreement.

In our model calculation we study the variance and power spectrum of the laser intensity $I_{\rm out}(t)$ transmitted with weak absorption through a cell of length $z = L$ for a given input stochastic light field whose statistics are specified at $z = 0$. For the input field we consider a phase-diffusing light field (PDF), a real Gaussian field (RGF), and a chaotic (or complex) Gaussian field (CGF). A PDF describes phase fluctuations of a well-stabilized single-mode laser, while a real Gaussian field corresponds to light with strong amplitude fluctuations and a locked phase. A complex Gaussian field describes the intermediate situation between these extremes since it has amplitude and correlated-phase fluctuations. Our theory is valid to all orders in the incident light field but we confine ourselves to the weak absorption limit.

The paper is organized as follows. In Sec. II we calculate the transmission of a time-dependent field through a medium of two-level systems. In Sec. II B we introduce the stochastic input fields and their correlation functions. Relevant observables such as the mean transmitted intensity, the variance, and power spectrum are defined in Sec. II C. Section III presents a discussion of the exact (numerical) and perturbative results for two-level atoms, while Sec. IV examines as an example the power spectrum of a phase-diffusing field interacting with a four-level medium corresponding to the experiment of Ref. [8].

II. ABSORPTION INDUCED INTENSITY FLUCTUATIONS: THE MODEL

A. Maxwell-Bloch equations

Propagation of a laser wave through a medium is described by the Maxwell-Bloch equations [10, 11]. In our

model we consider a one-dimensional situation with light propagating along the positive z direction and a medium extending from $z = 0$ to $z = L$. For the positive frequency part of the electric field we write

$$\mathbf{E}^{(+)}(z,t) = \epsilon(z,t)\,\boldsymbol{\varepsilon}\,\exp[-i(\omega t - kz)]. \tag{1}$$

Here $\epsilon(z,t)$ is a slowly varying complex field envelope, $\boldsymbol{\varepsilon}$ is a linear polarization vector, and ω and k denote the frequency and wave vector of the light, respectively. The source term in the Maxwell equation is proportional to the atomic polarization density $\mathbf{P}^{(+)}(z,t)$,

$$\mathbf{P}^{(+)}(z,t) = \left\{\mathcal{P}^{(+)}(z,t;v)\right\}_v \exp[-i(\omega t - kz)]. \tag{2}$$

For an inhomogeneously broadened medium we have to average the polarization over the Doppler distribution; this is indicated by the velocity average $\{\ldots\}_v = \int_{-\infty}^{\infty}(\ldots)K(v)\,dv$ with

$$K(v) = k/(\sqrt{\pi}D)\exp[-(kv/D)^2] \tag{3}$$

the Maxwell-Boltzmann distribution. The Doppler width D is related to the temperature of the gas by $D = \sqrt{2k_BT/m}$.

By formally integrating Maxwell's equation in the slowly varying envelope approximation, we relate the output field $\epsilon_{\text{out}}(t) \equiv \epsilon(z = L, t)$ and the input field $\epsilon_{\text{in}}(t) \equiv \epsilon(z = 0, t)$ through

$$\epsilon_{\text{out}}(t) = \epsilon_{\text{in}}(t_{ret}) + \frac{ik}{2\epsilon_0}\int_0^{z=L} dz'\{\boldsymbol{\varepsilon}^*\cdot\boldsymbol{\mathcal{P}}^{(+)}(z', t_{ret} + z'/c; v)\}_v, \tag{4}$$

with $t_{ret} = t - L/c$.

For a medium of two-level atoms with ground state $|0\rangle$ and excited states $|1\rangle$ the polarization density within a small volume dV containing $dN = n\,dV$ two-level atoms is

$$\boldsymbol{\mathcal{P}}^{(+)}(z,t;v)\,dV = 2\,\mathbf{D}_{01}\,\rho_{10}(z,t;v)\,dN \tag{5}$$

with $\mathbf{D}_{01}$ the atomic dipole between ground and excited states and $\rho_{10}(z,t;v)$ the slowly varying atomic coherences of a single atom moving with velocity v. In the absence of velocity-changing collisions or other mechanisms affecting the free linear motion of the atom the time evolution of the atomic density matrix is determined by the Bloch equations for a single moving system

$$\left[\left(\frac{\partial}{\partial t} + v\frac{\partial}{\partial z}\right) - \begin{pmatrix} \mathcal{Z} & 0 & i\frac{\Omega^*(z,t)}{2} & 0 \\ 0 & \mathcal{Z}^* & -i\frac{\Omega(z,t)}{2} & 0 \\ i\Omega(z,t) & -i\Omega^*(z,t) & -\kappa & -\kappa \\ 0 & 0 & 0 & 0 \end{pmatrix}\right]\begin{pmatrix} \rho_{01}(z,t;v) \\ \rho_{10}(z,t;v) \\ w(z,t;v) \\ \mathrm{tr}(z,t;v) \end{pmatrix} = 0\,, \tag{6}$$

with Rabi frequency $\Omega(z,t) = 2\boldsymbol{\varepsilon}\mathbf{D}_{10}\,\epsilon(z,t)/\hbar$, detuning $\delta = \omega - \omega_{10}$, the population inversion w, and the trace $\mathrm{tr} \equiv 1$. The Doppler shift is already included in $\mathcal{Z} = -i(\delta - kv) - \frac{\kappa}{2}$. The detailed form of $\boldsymbol{\mathcal{P}}^{(+)}(z,t;v)$ depends on the underlying atomic structure. In the present section, we have assumed that a two-level approximation is valid. A four-level configuration modeling ^{133}Cs is considered in Sec. IV.

In an optically thin medium, the difference between local and incident field is small and we use perturbation theory to solve the Maxwell-Bloch equations (6) and (4). We evaluate the polarization term in (4) by approximating the field $\epsilon(z,t)$ by the incident field, $\epsilon(z,t) \to \epsilon_{\text{in}}(t - z/c)$, and we find for the field at the end of the cell $z = L$

$$\epsilon_{\text{out}}(t) = \epsilon_{\text{in}}(t_{ret}) + i\,(\alpha L)\sqrt{\langle\langle\epsilon_{\text{in}}\epsilon_{\text{in}}^*\rangle\rangle} \times\{\rho_{10}(z=0, t_{ret}; v)\}_v + O((\alpha L)^2)\,, \tag{7}$$

with $(\alpha L) = n\,(kL)\boldsymbol{\varepsilon}^*\mathbf{D}_{01}/(\epsilon_0\langle\langle\epsilon_{\text{in}}\epsilon_{\text{in}}^*\rangle\rangle^{(1/2)})$ and the density of atoms n. At this stage, it is not necessary to introduce the mean incident, stationary, intensity $\langle\langle\epsilon_{\text{in}}\epsilon_{\text{in}}^*\rangle\rangle$ but it facilitates the further application to stochastic input fields and the definition of a dimension-free attenuation parameter (αL).

B. Models for stochastic input fields

The transmitted field $\epsilon_{\text{out}}(t)$ is determined by the incident field $\epsilon_{\text{in}}(t)$ and the atomic structure. Fluctuations and noise are inherited by $\epsilon_{\text{out}}(t)$. However, the noise is modified by the interaction and thus carries information on the atomic structure. In this paper, we consider three prototypical models for describing a stochastic $\epsilon_{\text{in}}(t)$: a phase-diffusion model (PDM), a complex Gaussian field, and a real Gaussian field. Their common features are the mean emitted intensity $\langle\langle\epsilon_{\text{in}}\epsilon_{\text{in}}^*\rangle\rangle$ and the bandwidth b of the associated spectrum which we assume to be Lorentzian. Although all models have the same autocorrelation function

$$g^{(1)}(\tau) = \lim_{t\to\infty}\frac{\langle\langle\epsilon_{\text{in}}^*(t)\epsilon_{\text{in}}(t+\tau)\rangle\rangle}{\langle\langle\epsilon_{\text{in}}^*(t)\epsilon_{\text{in}}(t)\rangle\rangle} = \exp(-b|\tau|), \tag{8}$$

they differ in their higher-order statistics

$$g^{(2)}(\tau) = \lim_{t\to\infty}\frac{\langle\langle\epsilon_{\text{in}}^*(t)\epsilon_{\text{in}}^*(t+\tau)\epsilon_{\text{in}}(t+\tau)\epsilon_{\text{in}}(t)\rangle\rangle}{\langle\langle\epsilon_{\text{in}}^*(t)\epsilon_{\text{in}}(t)\rangle\rangle^2} = 1 + \frac{(\Delta I)^2}{\langle\langle I\rangle\rangle^2}\exp(-2b|\tau|)\,. \tag{9}$$

The phase-diffusing field. According to the theory of a single-mode laser, which is operating above thresh-

old, the output field exhibits a slow diffusion of the phase and rapid (but small) fluctuations of the amplitude around a stationary mean value [12, 13]. The experimental fact that amplitude fluctuations are well suppressed in a diode laser [8, 14] supports the assumption that a phase-diffusion model is well suited to model fluctuations in semiconductor lasers.

The phase-diffusion model of the laser is described by phase fluctuations of the complex laser amplitude $\epsilon(t) = \epsilon_0\, e^{-i\phi(t)}$ where $\phi(t)$ is a Wiener process with zero mean, $\langle\langle d\phi(t)^2 \rangle\rangle = 2b\, dt$, and b is the Lorentzian bandwidth of the light. The PDF has no amplitude fluctuations, so that $g^{(2)}(\tau) = 1$.

The complex Gaussian field. A field generated by superposing a large number of independent, randomly phased, fields approaches a CGF [2]. The phase of the resulting field is random and the intensity fluctuations are as large as the mean intensity itself $(\Delta I)^2 = \langle\langle I \rangle\rangle^2$. Examples are thermal sources of radiation as well as multimode lasers with no phase-locking mechanism. A complex Gaussian field $\epsilon(t) = x(t) + i\, y(t)$ with Lorentzian spectrum and bandwidth b can be found as a solution of the Langevin equations

$$\begin{aligned} dx(t) &= -bx(t)\, dt + \sqrt{b\, \langle\langle \epsilon_{\rm in}\epsilon_{\rm in}^* \rangle\rangle}\, dW_1(t), \\ dy(t) &= -by(t)\, dt + \sqrt{b\, \langle\langle \epsilon_{\rm in}\epsilon_{\rm in}^* \rangle\rangle}\, dW_2(t), \end{aligned} \tag{10}$$

with noise increments obeying $\langle\langle dW_i(t)\, dW_j(t) \rangle\rangle = \delta_{ij}\, dt$ and $\langle\langle dW_i(t) \rangle\rangle = 0$. The intensity correlation function is given by $g^{(2)}(\tau) = 1 + 1\exp(-2b|\tau|)$.

The real Gaussian field. If a CGF is formed by two quadrature components fluctuating independently, a real Gaussian field [15] is characterized by two fully correlated quadrature components, i.e., the fluctuations are derived from the same source apart from some constant phase factor $\epsilon(t) = e^{-i\phi_0} x(t)$. The Langevin equation for the real field amplitude is

$$dx(t) = -bx(t)\, dt + \sqrt{2b\, \langle\langle \epsilon_{\rm in}\epsilon_{\rm in}^* \rangle\rangle}\, dW(t), \tag{11}$$

with $\langle\langle dW(t)^2 \rangle\rangle = dt$, $\langle\langle dW(t) \rangle\rangle = 0$. Since no phase fluctuations occur, there are increased intensity fluctuations with respect to the same mean intensity $(\Delta I)^2 = 2\, \langle\langle I \rangle\rangle^2$ and $g^{(2)}(\tau) = 1 + 2\exp(-2b|\tau|)$.

C. Output intensity fluctuations

The detected intensity at the end of the cell $z = L$ $I_{\rm out}(t) = 2c\epsilon_0\, \epsilon_{\rm out}(t)\epsilon_{\rm out}^*(t)$ is calculated from Eq. (7) and consists of several contributions of decreasing magnitude in (αL) :

$$I_{\rm out}(t) = I_{\rm in}(t_{ret}) + (\alpha L)\{I_{\rm abs}(t_{ret}; v)\}_v + O((\alpha L)^2). \tag{12}$$

The incident intensity is denoted by $I_{\rm in}$, $I_{\rm abs}$ is the absorbed intensity

$$I_{\rm abs}(t; v) = 2c\epsilon_0\, i\sqrt{\langle\langle \epsilon_{\rm in}\epsilon_{\rm in}^* \rangle\rangle}\, \epsilon_{\rm in}^*(t)\rho_{10}(z = 0, t; v) + \text{c.c.}, \tag{13}$$

and the errors due to approximations are of order $(\alpha L)^2$. After performing the stochastic average $\langle\langle \ldots \rangle\rangle$, we find the dominant contributions to the mean intensity and variance

$$\langle\langle I_{\rm out}(t) \rangle\rangle = \langle\langle I_{\rm in}(t_{ret}) \rangle\rangle + (\alpha L)\{\langle\langle I_{\rm abs}(t_{ret}; v) \rangle\rangle\}_v + O((\alpha L)^2), \tag{14}$$

$$[\Delta I_{\rm out}(t)]^2 = [\Delta I_{\rm in}(t_{ret})]^2 + 2(\alpha L)\{\langle\langle I_{\rm in}(t_{ret}), I_{\rm abs}(t_{ret}; v) \rangle\rangle\}_v + O((\alpha L)^2)\,, \tag{15}$$

where we have introduced the notation for the variance $[\Delta I(t)]^2 = \langle\langle I(t), I(t) \rangle\rangle = \langle\langle I(t)^2 \rangle\rangle - \langle\langle I(t) \rangle\rangle^2$. A stationary intensity-correlation spectrum is defined by

$$S_{1,2}(\nu) = \lim_{t\to\infty} 2\,\text{Re} \int_0^\infty e^{-i\nu\tau}\, \langle\langle I_1(t+\tau), I_2(t) \rangle\rangle\, d\tau, \tag{16}$$

where Re denotes the real part. In the case of general stochastic driving field, the output intensity-correlation spectrum is

$$S_{\rm out,out}(\nu) = S_{\rm in,in}(\nu) + (\alpha L)\{[S_{\rm in,abs}(\nu; v) + S_{\rm abs,in}(\nu; v)]\}_v + O((\alpha L)^2). \tag{17}$$

The situation is different for a field with pure phase fluctuations. Due to the fact that the intensity $I_{\rm in}(t)$ is a constant, all correlation functions $\langle\langle I_{\rm in}, I(t) \rangle\rangle$ vanish identically by definition. The variance is therefore given by

$$[\Delta I_{\rm out}(t)]^2 = (\alpha L)^2\{\langle\langle I_{\rm abs}(t_{ret}; v_1), I_{\rm abs}(t_{ret}; v_2) \rangle\rangle\}_{v_1, v_2} + O((\alpha L)^3). \tag{18}$$

Similarly one finds

$$S_{\rm out,out}(\nu) = (\alpha L)^2\{S_{\rm abs,abs}(\nu; v_1, v_2)\}_{v_1, v_2} + O((\alpha L)^3). \tag{19}$$

D. Evaluation of stochastic averages

The calculation of the output intensity and the power spectrum of the intensity fluctuations requires us to determine stochastic atom-field averages and correlation functions. For the PDF, the CGF, and the RGF the averages can be found analytically. The possibility of obtaining an exact solution can be traced back to the Markovian property of the stochastic fields. The composite atom-field system $\{u_\mu(t), \epsilon_{\rm in}(t)\}$ with $u_\mu(t)$ a vector of atomic density matrix elements (or bilinear expressions in the atomic density matrix elements) is again a Markov process.

In order to find the dominant contributions to the mean intensity and its noise, as well as to the power spectrum, we have to calculate averages in the form $\langle\langle \epsilon_{\rm in}(t)^m u_\mu(t) \epsilon_{\rm in}(\bar{t})^n \rangle\rangle$ for RGF, or more generally $\langle\langle \epsilon_{\rm in}(t)^a \epsilon_{\rm in}(t)^{*b} u_\mu(t) \epsilon_{\rm in}(\bar{t})^{\bar{a}} \epsilon_{\rm in}(\bar{t})^{*\bar{b}} \rangle\rangle$ if a complex Gaussian field is considered. This can be done by means of characteristic functions, Taylor expansions, and results always in second-order difference equations which are solved by matrix continued fractions. They are evaluated numerically with reasonable convergence properties.

However, all calculations involving a complex Gaussian field are algebraically more involved since there are correlated phase-amplitude fluctuations [16].

In the case of a PDF the evaluation is more easily accomplished since it can be done in closed form and no continued fractions are involved. It is sufficient to determine averages in the form $\langle\langle \epsilon_0 e^{-in\Phi(t)} u_\mu(t) \rangle\rangle$ and $\langle\langle \epsilon_0 e^{-in\Phi(t)} u_\mu(t), \epsilon_0 e^{im\Phi(\bar{t})} u_\nu(\bar{t})^* \rangle\rangle$, with $n, m = 0, \pm 1$.

The formalism we have used to calculate the averages and correlation functions is outlined in Appendix A for the RGF (the calculation for the CGF is very similar), and in Appendix B for the PDF (for details see also [5] and references cited).

III. RESULTS AND DISCUSSION

A. Mean intensity of the transmitted light

The mean intensity of the transmitted light shows the usual absorption profile with respect to detuning (see Fig. 1). For low intensities the linewidth is given by the natural linewidth (no other broadening mechanisms were considered) while with increasing saturation parameter $S = \Omega_{\rm in}^2/(\kappa b)$ [with $\Omega_{\rm in} = \langle\langle \Omega_{\rm in}(t)\Omega_{\rm in}(t)^* \rangle\rangle_{stat.}^{1/2}$] we have power broadening. In Fig. 1, $b = \kappa$ and $\Omega_{\rm in} = 10\kappa$, and the linewidth is therefore mainly determined by power broadening. The value of the dimensionless attenuation parameter was somewhat arbitrarily chosen as $(\alpha L) = 0.2$. The influence of the incident field statistics on the absorption profile is small. This can be understood qualitatively by studying the perturbation limit for weak saturation,

$$\rho_{01}(t; v) = \left(-\frac{i}{2}\right) \int_{-\infty}^{t} dt_1 \, e^{Z(t-t_1)} \Omega_{\rm in}^*(t_1). \tag{20}$$

Since $I_{\rm abs}(t; v)$ is proportional to $\mathrm{Im}\{\Omega_{\rm in}(t)\rho_{01}(t; v)\}$, we find for the transmitted intensity that

$$\langle\langle I_{\rm out} \rangle\rangle = \langle\langle I_{\rm in} \rangle\rangle \left(1 + (\alpha L) \langle\langle \Omega_{\rm in}\Omega_{\rm in}^* \rangle\rangle^{\frac{1}{2}} \mathrm{Re}\left\{ \frac{1}{Z - b} \right\}_v \right) + O((\alpha L)^2; \Omega_{\rm in}^2), \tag{21}$$

with $Z = -i(\delta - kv) - \kappa/2$. Within this approximation there is no influence of higher-order statistics since all three models of stochastic driving fields have the same first-order correlation functions.

The absorption dip scales proportional to D^{-1} in the case of inhomogeneous broadening $D \gg \kappa/2, b, \delta$, but no Doppler broadening was assumed in Fig. 1.

B. Induced intensity noise

We pointed out earlier that the noise in the transmitted intensity $(\Delta I_{\rm out})^2$ is a linear function of the attenuation parameter (αL) for fields with amplitude fluctuations (RGF,CGF), and goes quadratically in the case of a driving field with pure phase fluctuations (PDF).

1. The real and complex Gaussian field

It is instructive to study first the perturbative results for weak saturation. In this limit the fluctuations in the intensity $(\Delta I_{\rm out})^2$ are sensitive to the second-order field correlation functions of the incident light, $\langle\langle \epsilon_{\rm in}(t_1)\epsilon_{\rm in}^*(t_2)\epsilon_{\rm in}(t_3)\epsilon_{\rm in}^*(t_4) \rangle\rangle$. We find for the CGF

$$\begin{aligned}(\Delta I_{\rm out})^2_{(CGF)} &= \lim_{t\to\infty} \langle\langle I_{\rm in} \rangle\rangle^2 \\ &\quad \times \left(1 + 2\,(\alpha L) \langle\langle \Omega_{\rm in}\Omega_{\rm in}^* \rangle\rangle^{\frac{1}{2}} \mathrm{Re}\left\{ \frac{1}{Z - b} \right\}_v \right) \\ &\quad + O((\alpha L)^2; \Omega_{\rm in}^2) \\ &= \langle\langle I_{\rm out} \rangle\rangle^2 + O((\alpha L)^2; \Omega_{\rm in}^2),\end{aligned} \tag{22}$$

and for the RGF

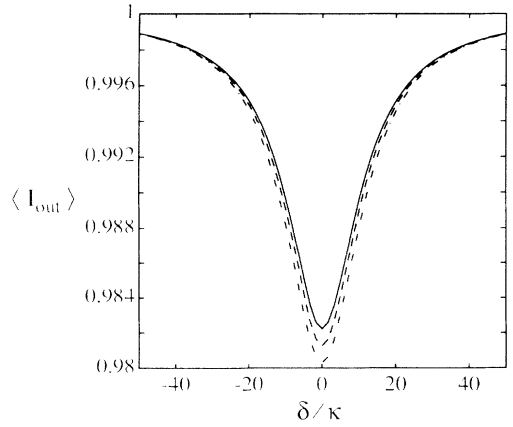

FIG. 1. Scaled mean transmitted intensity $\langle\langle I_{\rm out} \rangle\rangle / \langle\langle I_{\rm in} \rangle\rangle$ through a medium of two-level system for a real Gaussian field (solid), a complex Gaussian field (dashed), and a phase-diffusing field (dashed-dotted) vs detuning δ with $b = \kappa$, $\Omega_{\rm in} = 10\kappa$, $(\alpha L) = 0.2$, and no Doppler broadening, D=0.

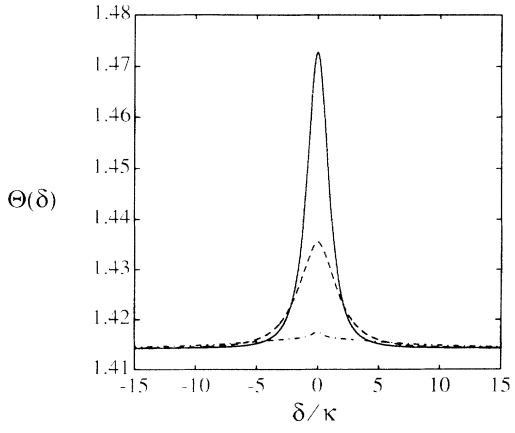

FIG. 2. Relative noise ratio $\Theta = \Delta I_{\rm out}/\langle\langle I_{\rm out} \rangle\rangle$ vs detuning for a real Gaussian driving field with $\Omega_{\rm in} = \kappa$, and increasing bandwidth: $b = 0.25\kappa$ (solid), $b = \kappa$ (dashed), and $b = 5\kappa$ (dashed dotted), $(\alpha L) = 0.2$. No Doppler broadening was assumed, D=0.

$$(\Delta I_{\rm out})^2_{(RGF)} = 2\,(\Delta I_{\rm out})^2_{(CGF)} = 2\,\langle\langle I_{\rm out}\rangle\rangle^2 + O((\alpha L)^2;\Omega^2_{\rm in})\,. \qquad (23)$$

Note that in this weak saturation limit there is no additional intensity noise caused by the propagation. Both the RGF and CGF retain their relative noise ratio $\Delta I_{\rm out}/\langle\langle I_{\rm out}\rangle\rangle = \Delta I_{\rm in}/\langle\langle I_{\rm in}\rangle\rangle + O[(\alpha L)^2;\Omega^2_{\rm in}]$. In the case of large inhomogeneous broadening, the absorption dip of $(\Delta I_{\rm out})^2$ decreases proportional to $D^{(-1)}$.

In Figs. 2 and 3 we plot our numerical results for the relative noise ratio $\Theta \equiv \Delta I_{\rm out}/\langle\langle I_{\rm out}\rangle\rangle + O[(\alpha L)^2]$. The individual curves represent Θ as a function of detuning for the three values of the saturation parameter $S = 0.2$, 1, and 4. The relative noise ratio Θ increases with the laser light intensity. The noise ratios for the RGF and CGF show a similar qualitative behavior. The RGF shows a sharp albeit small resonant feature near zero detuning which is absent for the CGF. The width of this resonance ($\approx \kappa/2$) is independent of the bandwidth of the driving field. A similar resonance has been found and explained in our previous work on population fluctuations in resonance fluorescence [5]. With increasing saturation parameter we find a broadening of the noise as a function of detuning.

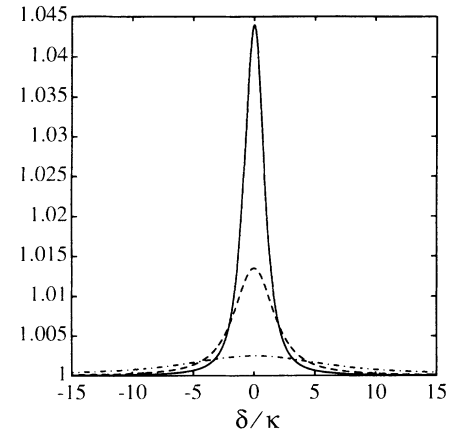

FIG. 3. Relative noise ratio Θ vs detuning for a complex Gaussian driving field. Same parameter values as in Fig. 2.

2. *The phase-diffusing field*

For an incident phase-diffusing field the intensity noise is generated by a transformation of phase fluctuations into amplitude fluctuations by the medium:

$$(\Delta I_{\rm out})^2_{(PDF)} = \lim_{t\to\infty}(\alpha L)^2\,\{\langle\langle I_{\rm abs}(t;v_1), I_{\rm abs}(t;v_2)\rangle\rangle\}_{v_1,v_2} + O((\alpha L)^3;\Omega^3_{\rm in})$$
$$= (\alpha L)^2\langle\langle I_{\rm in}\rangle\rangle^2\,2\,{\rm Re}\,\{\langle\langle \epsilon_{\rm in}(t)\rho_{01}(t;v_1), \epsilon^*_{\rm in}(t)\rho_{10}(t;v_2)\rangle\rangle - \langle\langle \epsilon_{\rm in}(t)\rho_{01}(t;v_1), \epsilon_{\rm in}(t)\rho_{01}(t;v_2)\rangle\rangle\}_{v_1,v_2}\,. \qquad (24)$$

The intensity noise decreases linearly as the bandwidth of the incident light becomes smaller than the atomic decay width. This was already demonstrated and explained in Ref. [9].

To see this we consider the weak saturation limit first and find that the two contributing correlation functions show a different behavior with respect to phase noise. The first correlation function is proportional to

$$\langle\langle \Omega_{\rm in}(t)\rho_{01}(t;v_1)\Omega_{\rm in}(t)^*\rho_{10}(t;v_2)\rangle\rangle = \langle\langle |\Omega_{\rm in}|^2\rangle\rangle\langle\langle \rho_{01}(t;v_1)\rho_{10}(t;v_2)\rangle\rangle$$
$$= \frac{\langle\langle |\Omega_{\rm in}|^2\rangle\rangle}{4}\int_{-\infty}^{t} dt_1 \int_{-\infty}^{t} dt_2\, e^{Z_1(t-t_1)+Z_2^*(t-t_2)}\langle\langle \Omega^*_{\rm in}(t_1)\Omega_{\rm in}(t_2)\rangle\rangle. \qquad (25)$$

It is rather insensitive to phase fluctuations and centered around $v_1 \approx v_2$. However, the second correlation function $\langle\langle \Omega_{\rm in}(t)\rho_{01}(t;v_1)\Omega_{\rm in}(t)\rho_{01}(t;v_2)\rangle\rangle$ is strongly influenced by phase noise but is also smaller in magnitude. This term is responsible for the noise maxima which appear if the bandwidth is small enough. From the final expression for the intensity noise

$$(\Delta I_{\rm out})^2_{(PDF)} = (\alpha L)^2\langle\langle I_{\rm in}\rangle\rangle^2\langle\langle \Omega_{\rm in}\Omega^*_{\rm in}\rangle\rangle \times {\rm Re}\,\{h(Z_1,Z_2)\}_{v_1,v_2} + O((\alpha L)^3;\Omega^3_{\rm in})\,, \qquad (26)$$

with

$$h(Z_1,Z_2) = -\frac{b}{Z_1-b}\left(\frac{1}{(Z_1+Z_2^*)(Z_2^*-b)} - \frac{1}{(Z_1+Z_2-4b)(Z_2-b)}\right) \qquad (27)$$

and $Z_1 = -i(\delta - kv_1) - \kappa/2$, $Z_2 = -i(\delta - kv_2) - \kappa/2$, we find that these noise maxima appear at $\delta = \pm\kappa/2$ if $b \ll \kappa$. In the case of large inhomogeneous broadening $D \gg b \gg \kappa$ all of these features vanish:

$$(\Delta I_{\rm out})^2_{(PDF)} \approx (\alpha L)^2\langle\langle I_{\rm in}\rangle\rangle^2\langle\langle \Omega_{\rm in}\Omega^*_{\rm in}\rangle\rangle\frac{\pi}{D^2} \times \exp\,[-2(\delta/D)^2]\,. \qquad (28)$$

In Fig. 4, we show the relative intensity noise ratio Θ of the output field for an arbitrarily strong field. The individual curves represent Θ as a function of detuning for an increasing bandwidth $b = 0.25\kappa$ (solid curve), $b = \kappa$ (dashed curve), $b = 5\kappa$ (dashed dotted curve); the corresponding saturation parameters are $S = 0.2$, 1, and 4. We note again the appearance of noise maxima off resonance. This feature remains well resolved as long as the bandwidth is smaller than the Rabi frequency. To understand this qualitatively, let us consider a field which has slow frequency fluctuations on the time scale given by the atomic decay: such a field experiences absorption

according to the absorption profile in Fig. 1 so that the conversion of frequency to amplitude fluctuations will be at a maximum for detunings near the points of maximal slope. For the corresponding discussion in the context of population fluctuations see Ref. [4].

C. Power spectrum of the transmitted intensity fluctuations

In this section we analyze the spectrum of the intensity fluctuations of the medium.

1. *The real and complex Gaussian field*

According to Eq. (17) the intensity-correlation spectrum for the transmitted field consists of three contributions: the sum of the first and the second term, $S_{\mathrm{in,in}} + S_{\mathrm{in,abs}}$, correlates the incident intensity and the transmitted light. These two terms lead to a frequency dependence in the form of a simple Lorentzian with bandwidth $2b$ (reflecting the spectrum of the incident laser). The third contribution, $S_{\mathrm{abs,in}}$, is a spectrum relating the absorbed intensity to the intensity of its driving field. This part of the spectrum exhibits resonances near the Rabi frequency. However, the output intensity spectrum is always dominated by $S_{\mathrm{in,in}}$. Thus we plot in Figs. 5 (RGF) and 6 (CGF) only the nontrivial part of the spectrum, defined by

$$S(\nu) = (S_{\mathrm{in,in}} - S_{\mathrm{out,out}})/\langle\langle I_{\mathrm{in}}\rangle\rangle^2 = -[S_{\mathrm{in,abs}}(\nu) + S_{\mathrm{abs,in}}(\nu)]/\langle\langle I_{\mathrm{in}}\rangle\rangle^2 . \tag{29}$$

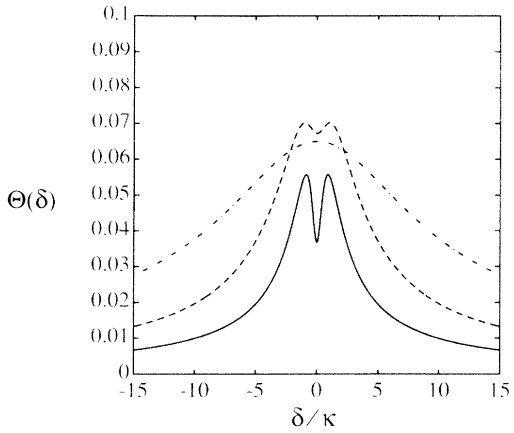

FIG. 4. Relative noise ratio $\Theta(\delta)$ vs detuning for a phase-diffusing driving field with $\Omega_{\mathrm{in}} = \kappa$, an increasing bandwidth: $b = 0.25\kappa$ (solid), $b = \kappa$ (dashed), $b = 5\kappa$ (dashed dotted), and $(\alpha L) = 0.2$. No Doppler broadening was assumed.

The two curves show $S(\nu)$ for a bandwidth of $b = \kappa$ and $b = 5\kappa$.

For b sufficiently small ($b = \kappa$) the Rabi sidebands of $S_{\mathrm{abs,in}}$ (in Figs. 5 and 6, $\Omega_{\mathrm{in}} = 10\kappa$) are dominated by the Lorentzian spectrum $S_{\mathrm{in,abs}}$. This behavior is found for strong and weak saturation intensities and can be seen explicitly in the following analytical expression derived in the limit of weak fields:

$$S^{(CGF)}_{\mathrm{out,out}}(\nu) = S^{(RGF)}_{\mathrm{out,out}}/2 = \mathrm{Re}\left\{ \frac{2}{i\nu + 2b} \left[(\Delta I_{\mathrm{out}})^2_{(CGF)} - (\alpha L)\langle\langle \Omega_{\mathrm{in}}\Omega^*_{\mathrm{in}}\rangle\rangle^{\frac{1}{2}} \langle\langle I_{\mathrm{in}}\rangle\rangle^2 \times \left(\frac{b}{(Z-b)(Z-b-i\nu)} + \frac{b}{(Z^*-b)(Z^*-b-i\nu)} \right) \right] \right\}_v + O((\alpha L)^2; \Omega^2_{\mathrm{in}}) . \tag{30}$$

In Fig. 6, the Rabi sidebands are still visible for the CGF ($b = \kappa$). By increasing the bandwidth $b = 5\kappa$ the contribution from the central Lorentzian spectrum decreases and the Rabi sidebands become clearly visible. The spectrum for the CGF is always smaller in magnitude than the spectrum for the RGF, but the qualitative features are the same.

By studying the weak saturation expansion for S_{out} for large inhomogeneous broadening $D \gg b \gg \kappa$ we find that the Rabi sidebands $S_{\mathrm{abs,in}}$ scale as $D^{(-2)}$ and $S_{\mathrm{in,abs}}$ goes as $D^{(-1)}$; $S_{\mathrm{in,in}}$ remains unaffected by the Doppler average.

2. *The phase-diffusing field*

The intensity fluctuations and the power spectrum for the PDF are of order $(\alpha L)^2$. We find, however, that the peak at the Rabi frequency is much more pronounced than for the RGF or CGF. This can be seen in Fig. 7, which shows the intensity-correlation spectrum as a function of frequency ν. The individual curves represent $S_{\mathrm{out,out}}$ for $b = \kappa$ (solid line), $b = 5\kappa$ (dashed line). The Rabi frequency is $\Omega_{\mathrm{in}} = 10\kappa$. The weak saturation expansion for the spectrum,

$$S_{\mathrm{out,out}}(\nu) = (\alpha L)^2 \langle\langle I_{\mathrm{in}}\rangle\rangle^2 \langle\langle \Omega_{\mathrm{in}}\Omega^*_{\mathrm{in}}\rangle\rangle \mathrm{Re}\left\{ h(Z_1, Z_2) \left(\frac{1}{i\nu + b - Z_1} + \frac{1}{-i\nu + b - Z_1} \right) \right\}_{v_1, v_2} + O((\alpha L)^3; \Omega^3_{\mathrm{in}}) , \tag{31}$$

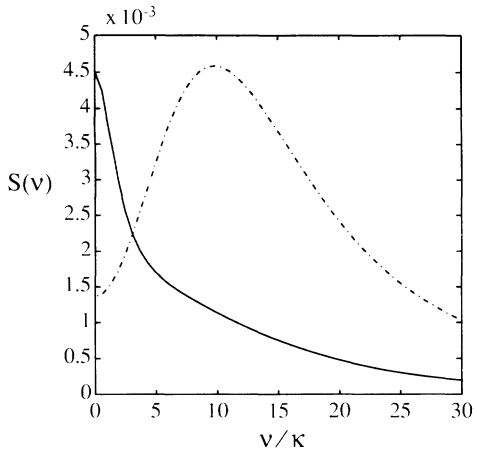

FIG. 5. Intensity-correlation spectrum for a real Gaussian field. Only the nontrivial part of the spectrum, $S(\nu) = [S_{\mathrm{in,in}}(\nu) - S_{\mathrm{out,out}}(\nu)]/\langle\langle I_{\mathrm{in}}\rangle\rangle^2$ is shown. The parameters are $\Omega_{\mathrm{in}} = 10\kappa$, $\delta = 0$, and $b = \kappa$ (solid line) and $b = 5\kappa$ (dashed dotted line). No Doppler broadening or detuning was assumed, $D = 0$.

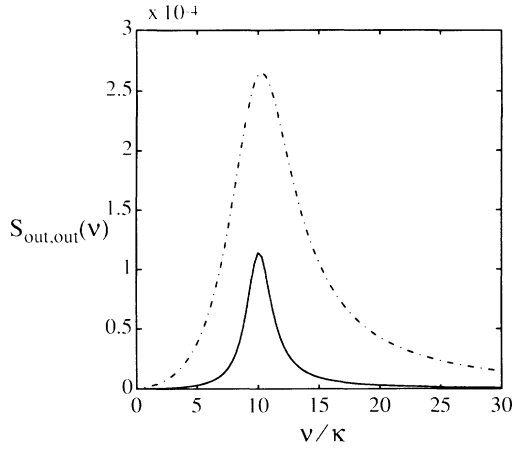

FIG. 7. Intensity-correlation spectrum for a phase-diffusing field $S_{\mathrm{out,out}}(\nu)/\langle\langle I_{\mathrm{in}}\rangle\rangle^2$ with $\Omega_{\mathrm{in}} = 10\kappa$, an increasing bandwidth $b = 1\kappa$ (solid), $b = 5\kappa$ (dashed dotted), and $(\alpha L) = 0.2$. No Doppler broadening or detuning was assumed, $D = 0, \delta = 0$.

is closely related to the variance of the intensity $(\Delta I_{\mathrm{out}})^2_{(PDF)}$ [see Eq. (24)]. These resonances are located at the generalized Rabi frequencies $\nu = \pm\delta$.

We have studied large inhomogeneous broadening $D \gg b, \delta, \kappa, \nu$ in this perturbative expression (31). In the limit of an arbitrarily large Doppler width we can replace the Doppler average $\int_{-\infty}^{\infty}(\ldots)K(v)dv$ by $K(v = 0)\int_{-\infty}^{\infty}(\ldots)dv$, and we are able to show by contour integration that this integral vanishes identically. More generally, we have found by asymptotic methods as well as numerical studies that the leading nonvanishing term in $S_{\mathrm{out,out}}(\nu)$ scales proportional to $D^{(-3)}$.

The strong saturation limit proves to be more interesting. By numerically integrating the exact intensity-correlation spectrum $S_{\mathrm{out,out}}(\nu)$ [see Eq. (B8)] we find that the overall scaling factor for the spectrum is now proportional to D^{-1}. Thus inhomogeneous broadening in the strong field limit will not wash out the features as for low intensities. In addition the resonance remains well resolved. In Fig. 8 we show the result of Doppler averaging $S_{\mathrm{out,out}}$ of Fig. 7. We have used a Doppler width of $D = 40\kappa$.

IV. SPECTROSCOPY OF ^{133}Cs WITH A PHASE-DIFFUSING LASER FIELD

In a recent article Yabuzaki *et al.* [8] reported a new type of intensity noise spectroscopy. They performed an absorption measurement in a vapor cell filled with ^{133}Cs atoms and observed that the intensity of the incident laser beam became quite noisy after having passed the

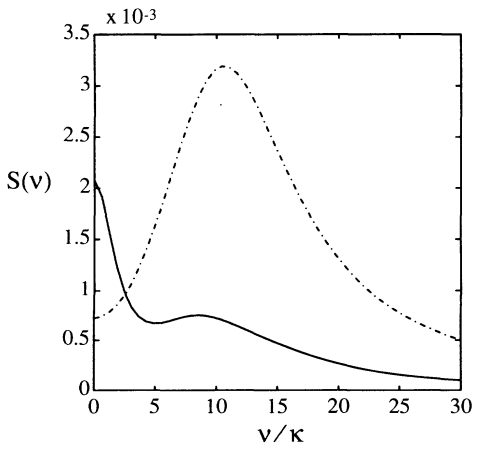

FIG. 6. Intensity-correlation spectrum for a complex Gaussian field. The parameters are the same as in Fig. 5.

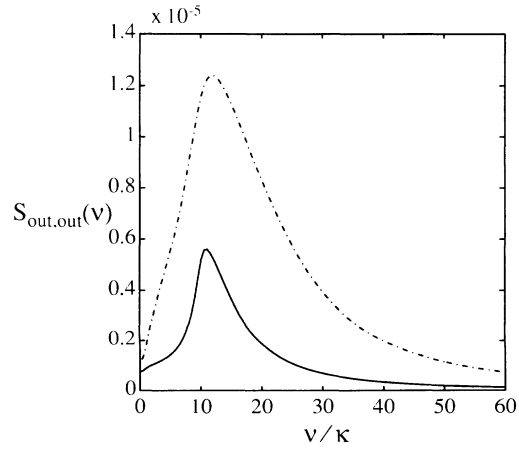

FIG. 8. Intensity-correlation spectrum for a phase-diffusing field $S_{\mathrm{out,out}}(\nu)/\langle\langle I_{\mathrm{in}}\rangle\rangle^2$. Same parameters as in Fig. 7 but a Doppler width of $D = 40\kappa$.

cell. For this experiment they employed a commercial Fabry-Pérot type diode laser whose amplitude is in general very stable (amplitude fluctuations are reported to be even below shot-noise limit [14]), however, the phase is fluctuating randomly. The width of the associated spectral line is typically tens of MHz. Among other results, they also reported a measurement of the hyperfine splitting of the D_2 transition of ^{133}Cs.

In this section we will demonstrate how to apply our theory to this multilevel system. In particular, we will calculate the intensity-correlation spectrum and relate the spectroscopy of the atom to the features in this noise spectrum. The calculation is based on the assumption that the laser field can be described by a PDF and thus has a Lorentzian spectrum with bandwidth b. In our calculations we have not included Doppler broadening.

We are interested in the ^{133}Cs $6S_{1/2}$ to $6P_{3/2}$ transition. The nuclear spin of this isotope is $I = 7/2$. Consequently we have four hyperfine states $F = 2, 3, 4, 5$ for the excited state separated by 150, 200, and 250 MHz, and two $F = 3, 4$ ground states with 9.2 GHz splitting. Below we consider the four-level system shown in Fig. 9. We will label these states starting from the bottom by $|0\rangle$, $|1\rangle$, $|2\rangle$, and $|3\rangle$. In our model calculations we ignore the Zeeman substructure.

The slowly varying envelope of the positive frequency part of the polarization [compare Eq. (5)] is in the present case given by

$$\boldsymbol{\mathcal{P}}^{(+)}(z,t)dV = 2\left[\mathbf{D}_{01}\,\rho_{10}(z,t) + \mathbf{D}_{02}\,\rho_{20}(z,t) + \mathbf{D}_{03}\,\rho_{30}(z,t)\right]dN \tag{32}$$

and it is straightforward to derive the corresponding atomic density matrix equations [17]. Consistent with the experiments we will further assume that the transition $|0\rangle \rightarrow |3\rangle$ is almost resonant with the incident light, i.e., the detuning $\delta_3 = \omega - \omega_{30}$ is much smaller than the level splittings ω_{32}, ω_{21}. Thus we can neglect the populations of the nonresonant levels. This gives us the two-level Bloch equations for the transition $|0\rangle$ - $|3\rangle$, and a set of equations for the coherences on the nonresonant transitions. The two-level equations are

$$\frac{d}{dt}\rho_{00} = \kappa_{30}\,\rho_{33} - i\frac{\Omega_3(t)}{2}\rho_{03} + i\frac{\Omega_3^*(t)}{2}\rho_{30}\ , \tag{33}$$

$$\frac{d}{dt}\rho_{03} = Z_3\,\rho_{03} + i\frac{\Omega_3^*(t)}{2}\left(\rho_{33} - \rho_{00}\right)\ , \tag{34}$$

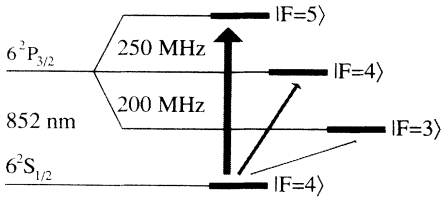

FIG. 9. Level scheme of ^{133}Cs within the D_2 transition ($6S_{J=1/2} \leftrightarrow 6P_{J=3/2}$).

$$\frac{d}{dt}\rho_{33} = -\kappa_{30}\,\rho_{33} + i\frac{\Omega_3(t)}{2}\rho_{03} - i\frac{\Omega_3^*(t)}{2}\rho_{30}\ , \tag{35}$$

with $Z_3 = -i\delta_3 - \kappa_{30}/2$, spontaneous decay rates κ_{j0}, and $\Omega_j(t) = 2\,\boldsymbol{\epsilon}\mathbf{D}_{j0}\,\epsilon(t)/\hbar$. This system has been discussed in the previous sections. The equations for the coherences are

$$\frac{d}{dt}\rho_{02} = Z_2\,\rho_{02} + i\frac{\Omega_3^*(t)}{2}\rho_{32} - i\frac{\Omega_2^*(t)}{2}\rho_{00}, \tag{36}$$

$$\frac{d}{dt}\rho_{32} = \left(-i\omega_{32} - \frac{\kappa_{20}+\kappa_{30}}{2}\right)\rho_{32} + i\frac{\Omega_3(t)}{2}\rho_{02}, \tag{37}$$

and

$$\frac{d}{dt}\rho_{01} = Z_1\,\rho_{01} + i\frac{\Omega_3^*(t)}{2}\rho_{31} - i\frac{\Omega_1^*(t)}{2}\rho_{00}, \tag{38}$$

$$\frac{d}{dt}\rho_{31} = \left(-i\omega_{31} - \frac{\kappa_{10}+\kappa_{30}}{2}\right)\rho_{31} + i\frac{\Omega_3(t)}{2}\rho_{01}, \tag{39}$$

with $Z_2 = -i\omega_{32} - i\delta_3 - \kappa_{20}/2$ and $Z_1 = -i\omega_{31} - i\delta_3 - \kappa_{10}/2$. The transmitted field [see Eq. (4)] and output intensity [see Eq. (12)] are calculated as in the previous sections,

$$I_{\rm out}(t) = I_{\rm in} + \sum_{l=1}^{3}(\alpha_l L) I_{{\rm abs}(l)}(t_{ret}) + O[(\alpha_i L)(\alpha_j L)]\ , \tag{40}$$

with $(\alpha_i L) = n\,(kL)\boldsymbol{\epsilon}^*\mathbf{D}_{0i}/(\epsilon_0\langle\langle\epsilon_{\rm in}\epsilon_{\rm in}^*\rangle\rangle^{1/2})$ and n the atomic density.

In the following we will focus on the discussion of the intensity-correlation spectrum, since it contains all the physical information about position and width of the transitions as well as saturation effects. The power spectrum of the transmitted field is given by the expression

$$\begin{aligned} S_{\rm out,out}(\nu) &= \sum_{l=1}^{3} S_{{\rm abs}(l),{\rm out}}(\nu) + O((\alpha L)^3) \\ &= \sum_{l=1}^{3}\lim_{t\to\infty} 2\,{\rm Re}\int_0^\infty e^{-i\nu\tau}\sum_{j=1}^{3}\left\langle\left\langle(\alpha_l L) I_{{\rm abs}(l)}(t+\tau), (\alpha_j L) I_{{\rm abs}(j)}(t)\right\rangle\right\rangle d\tau + O((\alpha L)^3)\ , \end{aligned} \tag{41}$$

where the subscripts l and j indicate summation over all excited states. For a fixed l the partial spectrum $S_{{\rm abs}(l),{\rm out}}$ consists of two resonances whose locations are determined by the beat frequency of the incident field ω and the dipole oscillation frequency ω_{l0}. In our example these resonances occur at $\nu = \pm\delta_3$, $\pm(\omega_{32}+\delta_3)$, and $\pm(\omega_{31}+\delta_3)$. This can be most easily seen from Eqs. (34), (36), and (38) for ρ_{0l} when we neglect the depletion of the ground state as well as the time dependence of the Rabi frequency (i.e., ignore the bandwidth). Then

$I_{\mathrm{abs}(l)}(t)$ is proportional to $|\Omega_l|\mathrm{Im}\rho_{0l}(t)$ and the Fourier transform will exhibit these beat frequencies. Observation of the resonances in the noise spectrum thus allows one to determine the splitting frequencies of the excited states.

To study the width of the resonances we have to include the stochastic temporal behavior of the Rabi frequency (phase noise). In the weak saturation regime we can simply relate the power spectrum to the fourth-order correlation function of the incident field and find

$$S_{\mathrm{out,out}}(\nu) = \langle\langle I_{\mathrm{in}}\rangle\rangle^2 \mathrm{Re}\sum_{l=1}^{3}(\alpha_l L)s_l\left(\frac{1}{i\nu+b-Z_l} + \frac{1}{-i\nu+b-Z_l}\right) + O((\alpha L)^3;\Omega_{\mathrm{in}}) , \quad (42)$$

with

$$s_l = \sum_{j=1}^{3}(\alpha_j L)\langle\langle\Omega_l\Omega_j^*\rangle\rangle h(Z_l,Z_j)$$

[compare Eq. (31)]. This shows now the position, width, and strength of the six resonances at the complex frequencies $\nu_3 = \pm\delta_3 - i(\kappa_{30}/2+b)$, $\nu_2 = \pm(\omega_{32}+\delta_3) - i(\kappa_{20}/2+b)$, and $\nu_1 = \pm(\omega_{31}+\delta_3) - i(\kappa_{10}/2+b)$.

We have performed numerical calculations valid in the strong saturation regime. In Fig. 10 we plot the power spectrum $S_{\mathrm{out,out}}(\nu)$ for a saturating field $\Omega_{j=1,2,3} = 4\kappa$ which is resonant with the $|0\rangle$-$|3\rangle$ transition and has a bandwidth $b = 3\kappa$. When this is compared to Fig. 3 of Ref. [8] we see that we get good qualitative agreement with the experimental results. Since the laser in Ref. [8] was roughly tuned to the $^2S_{1/2}, F' = 4 \leftrightarrow {}^2P_{3/2}, F = 5$ transition they observed resonances at $\nu_1 = \omega_{F=5,F=3} = 453$ MHz and $\nu_2 = \omega_{F=5,F=4} = 251$ MHz. From these frequencies as well as their differences $\nu_2 - \nu_1 = \omega_{F=4,F=3} = 202$ MHz one can determine the hyperfine splitting of the $6^2P_{3/2}$ states $|F=5\rangle$, $|F=4\rangle$, and $|F=3\rangle$ from the intensity noise spectrum.

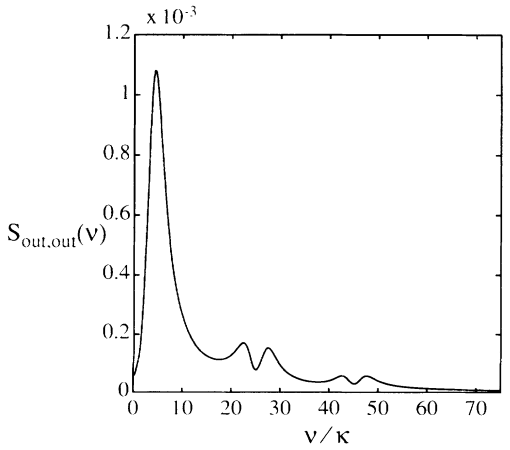

FIG. 10. Intensity-correlation spectrum for ^{133}Cs with $b = 3\kappa$, $\Omega_1 = \Omega_2 = \Omega_3 = 4\kappa$, $\delta_3 = 0$, $\omega_{31} = 45\kappa$, $\omega_{32} = 25\kappa$, and $(\alpha_{(1,2,3)}L) = 0.2$. No Doppler broadening was assumed, $D = 0$.

In comparing our results with experiments we point out, however, that the splitting observed in the experimental spectrum is caused by hole burning due to inhomogeneous broadening (Doppler effects are ignored in our treatment), while the origin of the splitting in our spectrum (Fig. 10) is that all three transitions are excited by the same saturating field. Therefore the atom will end up in a superposition state where coherences between excited states become important. Again this can be understood qualitatively by assuming that $\Omega_l(t)$ is constant on the atomic time scales (i.e., we ignore the phase fluctuations). Hence $I_{\mathrm{abs}(l)}(t)$ is proportional to $|\Omega_l|\mathrm{Im}\rho_{0l}$. Under the influence of a strong field ρ_{02} is coupled to the coherence ρ_{32} and vice versa. By examining the homogeneous part of Eqs. (36) and (37) one finds that the resonance frequency of ρ_{02}: $\nu = \omega_{32} + \delta_3$ splits up into $\nu = \omega_{32} + \delta_3 \pm |\Omega_3|/2$. The same arguments apply to the other transition. From Fig. 10 we see that this qualitative argument is still valid for finite bandwidth.

V. CONCLUSIONS

In this paper we have studied the change in statistics of a laser propagating through a weakly absorbing medium. In particular we have been interested in the change of intensity fluctuations and the intensity power spectrum. As a model for classical stochastic input fields we have considered a phase-diffusing field, and a real and complex Gaussian field. These models have the same light spectrum (Lorentzian with bandwidth b) but differ in their higher-order correlation functions.

Our analysis has shown that the power spectrum and the variance of the output intensity scales proportional to the absorption length for amplitude modulated fields while it goes quadratically for fields with phase noise. Comparing $\Delta I_{\mathrm{out}}/\langle\langle I_{\mathrm{out}}\rangle\rangle$ as a function of detuning for different noise fields and a two-level atom, we found that this ratio is always maximum on resonance for fields with amplitude fluctuations (RGF, CFG) while in the case of a PDF there can be a local minimum if the bandwidth is sufficiently small. The power spectra for fields with amplitude fluctuations consist—apart from trivial zeroth-order contributions—of two first-order heterodyne spectra. The first of these terms reflects the stochastic properties of the incident intensity and has the form of a simple Lorentzian (vs spectral frequency) centered at the origin with a bandwidth of $2b$. The second contribution, however, reflects the dynamic response of the medium to the incident field and has a resonance at the generalized Rabi frequency. The Lorentzian part always dominates for small bandwidth, and this resonance becomes visible only for large bandwidths and Rabi frequencies. In contrast, for a PDF this resonance at the Rabi frequency is always much more pronounced. We have extended the theory to describe four-level systems corresponding to the noise spectroscopy experiment with Cs of Ref. [8] and found qualitative agreement with experimental results. An interesting new feature is the prediction that the resonances of the power spectrum which are associated with given transitions split in the strong field limit due to the coherent excitation of different levels.

ACKNOWLEDGMENTS

We thank Professor J. Cooper for discussions. This work has been supported in part by the National Science Foundation through grants to the University of Colorado.

APPENDIX A: A REAL GAUSSIAN FIELD

We outline the evaluation of the required equal-time ($t = \bar{t}$) stochastic averages in the case of a real Gaussian driving field. Moreover, we consider all bilinear atomic averages, since all linear averages are included as a special case [$u_4(t) = \mathrm{tr}(\rho) = 1$] and a simultaneous evaluation of resonance-fluorescence intensity [5] is then also possible:

$$\underline{\mathrm{g}}_2(\lambda,t) = \left\langle\!\left\langle e^{-i\lambda\tilde{\epsilon}(t)}\mathbf{u}(t)\mathbf{u}(t)^\top \right\rangle\!\right\rangle = e^{-\frac{\lambda^2}{2}} \sum_{n=0}^{\infty} \underline{\mathrm{g}}_2^{(n)}(t)\,\lambda^n\,, \tag{A1}$$

where we use a scaled $\tilde{\epsilon}(t) = \epsilon(t)/\sqrt{\langle\!\langle \epsilon\epsilon^* \rangle\!\rangle}$. Once the matrix coefficients $\underline{\mathrm{g}}_2^{(n)}(t)$ are found

$$\langle\!\langle \epsilon(t)^n \mathbf{u}(t)\mathbf{u}(t)^\top \rangle\!\rangle = \langle\!\langle \epsilon\epsilon^* \rangle\!\rangle^{\frac{n}{2}}\; i^n\, n! \times \sum_{j=0}^{[n/2]} \left(-\frac{1}{2}\right)^j \frac{1}{j!}\, \underline{\mathrm{g}}_2^{(n-2j)}(t), \tag{A2}$$

where $[n/2]$ is the greatest integer less than or equal to $n/2$.

The stochastic equation for the composite atom-field system $\{\mathbf{u}, \epsilon\}$, i.e., the Bloch equation, Eq. (6),

$$\frac{d}{dt}\mathbf{u}(t) = [\underline{\mathrm{A}} + \epsilon(t)\,\underline{\mathrm{B}}]\,\mathbf{u} \tag{A3}$$

and the stochastic field equation [see Eq. (11)] can be translated into an equation for the probability of a certain realization $P(\mathbf{u}, \epsilon, t)$

$$\left(\frac{\partial}{\partial t} + L(\epsilon)\right) P(\mathbf{u}, \epsilon, t|\bar{\mathbf{u}}, \bar{\epsilon}, \bar{t}) = -\nabla_{\mathbf{u}} \{(\underline{\mathrm{A}} + \epsilon(t)\,\underline{\mathrm{B}})\,\mathbf{u}P\}\,. \tag{A4}$$

In order to find the matrix coefficients $\underline{\mathrm{g}}_2^{(n)}(t)$, we have to use Eq. (A4) and solve

$$\begin{aligned}\frac{\partial}{\partial t}\underline{\mathrm{g}}_2^{(n)}(t) = &-nb\underline{\mathrm{g}}_2^{(n)} + \underline{\mathrm{A}}\underline{\mathrm{g}}_2^{(n)} + \underline{\mathrm{g}}_2^{(n)}\underline{\mathrm{A}}^\top \\ &+i\underline{\mathrm{B}}[(n+1)\underline{\mathrm{g}}_2^{(n+1)} - \underline{\mathrm{g}}_2^{(n-1)}] \\ &+i[(n+1)\underline{\mathrm{g}}_2^{(n+1)} - \underline{\mathrm{g}}_2^{(n-1)}]\underline{\mathrm{B}}^\top\,.\end{aligned} \tag{A5}$$

Once stationarity has been reached, we face a linear, homogeneous, second-order set of difference equations. Its solution can be found easily by using a linear isomorphism $\mathcal{F}$, which induces the so-called Kronecker or direct tensor product $\times$ by

$$\mathcal{F}\left(\underline{\mathrm{A}}\underline{\mathrm{g}}\underline{\mathrm{B}}^\top\right) = \underline{\mathrm{B}} \times \underline{\mathrm{A}}\,\mathcal{F}(\underline{\mathrm{g}})\,. \tag{A6}$$

Applying this to Eq. (A5), once stationarity has been reached, yields

$$\begin{aligned}\underline{0} &= (-n\,b\,\underline{1}\times\underline{1} + \underline{1}\times\underline{\mathrm{A}} + \underline{\mathrm{A}}\times\underline{1})\,\mathcal{F}(\underline{\mathrm{g}}_2^{(n)}) \\ &\quad + i\,(\underline{1}\times\underline{\mathrm{B}} + \underline{\mathrm{B}}\times\underline{1})\,[(n+1)\mathcal{F}(\underline{\mathrm{g}}_2^{(n+1)}) - \mathcal{F}(\underline{\mathrm{g}}_2^{(n-1)})] \\ &= \underline{\mathrm{Q}}_n\mathcal{F}(\underline{\mathrm{g}}_2^{(n)}) + \underline{\mathrm{Q}}_n^{(+)}\mathcal{F}(\underline{\mathrm{g}}_2^{(n+1)}) + \underline{\mathrm{Q}}_n^{(-)}\mathcal{F}(\underline{\mathrm{g}}_2^{(n-1)})\,.\end{aligned} \tag{A7}$$

This equation is now solved by a matrix continued fraction and

$$\underline{\mathrm{g}}_2^{(0)} = \mathbf{e}_4 \otimes \mathbf{e}_4 - \mathcal{F}^{-1}[(\underline{\mathrm{Q}}_0 + \underline{\mathrm{Q}}_0^{(+)}\underline{\mathrm{S}}_0^{(+)})^{-1}\underline{\mathrm{Q}}_0\mathcal{F}(\mathbf{e}_4 \otimes \mathbf{e}_4)] \tag{A8}$$

with

$$\underline{\mathrm{S}}_{n-1}^{(+)} = -(\underline{\mathrm{Q}}_n + \underline{\mathrm{Q}}_n^{(+)}\underline{\mathrm{S}}_n^{(+)})^{-1}\underline{\mathrm{Q}}_n^{(-)}\,. \tag{A9}$$

APPENDIX B: THE PHASE-DIFFUSING FIELD

If an atomic system is driven by a phase-diffusing field, all averages can be determined in closed form. We demonstrate it for the mean absorbed intensity $\langle\!\langle I_{\mathrm{abs}}(t;v) \rangle\!\rangle$ which is proportional to $\mathrm{Im}\langle\!\langle \epsilon_{\mathrm{in}}(t)\rho_{01}(t;v) \rangle\!\rangle$. The stochastic Bloch equation (6) is of the general form

$$\begin{aligned}d\mathbf{u}(t;v) &= \underline{\mathrm{A}}[\epsilon_{\mathrm{in}}(t) = \epsilon_0 e^{-i\Phi(t)}; v]\mathbf{u}(t;v)\,dt \\ &= \exp\left[-i\underline{\mathrm{N}}_0\Phi(t)\right]\underline{\mathrm{A}}\,(\epsilon_0; v) \\ &\quad \times \exp\left[i\underline{\mathrm{N}}_0\Phi(t)\right]\mathbf{u}(t;v)\,dt\,,\end{aligned} \tag{B1}$$

with $\langle\!\langle d\Phi(t)^2 \rangle\!\rangle = 2b\,dt$ a Wiener process and $\underline{\mathrm{N}}_0$ a diagonal matrix with integer elements. Introducing

$$\mathbf{g}_1(t;v) = \exp\left[i\underline{\mathrm{N}}_0\Phi(t)\right]\mathbf{u}(t;v) \tag{B2}$$

we obtain the required $\mathrm{Im}\langle\!\langle \epsilon_{\mathrm{in}}(t)\rho_{01}(t;v) \rangle\!\rangle$ as $\epsilon_0 \mathrm{Im}\,\langle\!\langle \mathbf{g}_1(t;v) \rangle\!\rangle_{\mu=1}$. The stochastic equation for $\mathbf{g}_1$ is

$$\begin{aligned}d\mathbf{g}_1(t;v) = &\exp\left\{i\underline{\mathrm{N}}_0\,[\Phi(t) + d\Phi(t)]\right\}\,[\mathbf{u}(t;v) + d\mathbf{u}(t;v)] \\ &- \exp\left[i\underline{\mathrm{N}}_0\Phi(t)\right]\mathbf{u}(t;v)\,.\end{aligned} \tag{B3}$$

According to the rules of Ito's calculus [16], we have to expand the exponent up to second order in $d\Phi(t)$, and make use of Eq. (B1) and the property of a Wiener increment. Since $\mathbf{u}(t)$ is nonanticipating, i.e., fluctuations in $\mathbf{u}(t)$ are not correlated with future noise $\langle\!\langle d\Phi(t)\mathbf{u}(t) \rangle\!\rangle = 0$. Consequently, we find the ordinary differential equation for $\langle\!\langle \mathbf{g}_1(t;v) \rangle\!\rangle$,

$$d\,\langle\!\langle \mathbf{g}_1(t;v) \rangle\!\rangle = \left[\underline{\mathrm{A}}\,(\epsilon_0; v) - b\,\underline{\mathrm{N}}_0{}^2\right]\,\langle\!\langle \mathbf{g}_1(t;v) \rangle\!\rangle\,dt\,. \tag{B4}$$

Second-order correlations $\mathbf{g}_2(t,t;v)$ can be treated similarly. It can even be generalized, if we consider two atoms, members of different velocity groups, that experience the same stochastic field but are detuned differently due to their various Doppler shifts.

$$\begin{aligned}\mathbf{g}_2(t,t;v_1,v_2) = &\exp\left[i\underline{\mathrm{N}}_0\Phi(t)\right]\mathbf{u}(t;v_1)\,\mathbf{u}^\dagger(t;v_2) \\ &\times \exp\left[-i\underline{\mathrm{N}}_0\Phi(t)\right].\end{aligned} \tag{B5}$$

$$\begin{aligned}d\,\langle\!\langle \mathbf{g}_2(t,t;v_1,v_2) \rangle\!\rangle = &\{\left[\underline{\mathrm{A}}\,(\epsilon_0,v_1) - b\,\underline{\mathrm{N}}_0^2\right]\langle\!\langle \mathbf{g}_2 \rangle\!\rangle \\ &+ \langle\!\langle \mathbf{g}_2 \rangle\!\rangle[\underline{\mathrm{A}}^\dagger\,(\epsilon_0,v_2) - b\,\underline{\mathrm{N}}_0^2] \\ &+2b\,\underline{\mathrm{N}}_0\,\langle\!\langle \mathbf{g}_2 \rangle\!\rangle\,\underline{\mathrm{N}}_0\}\,dt\,.\end{aligned} \tag{B6}$$

The covariance matrix is obtained by removing the mean values

$$\mathbf{c}_2(t,t;v_1,v_2) = \mathbf{g}_2(t,t;v_1,v_2) - \mathbf{g}_1(t;v_1)\,\langle\langle \mathbf{g}_1(t;v_2)\rangle\rangle^{\dagger} . \tag{B7}$$

Insights into the atomic dynamic and the influences of noise are gained by studying the correlation function $\langle\langle \mathbf{c}_2(\bar{t},t;v_1,v_2)\rangle\rangle$ with unequal-time arguments. Most conveniently it is studied in frequency domain. Laplace transformation $\mathcal{L}_s\{\langle\langle \mathbf{c}_2(\bar{t},t;v_1,v_2)\rangle\rangle\}$ is equivalent to Fourier transformation once stationarity has been reached:

$$\langle\langle \mathbf{c}_2(s=i\nu;v_1,v_2)\rangle\rangle = \lim_{t\to\infty}\left\{i\nu - \left[\underline{\mathrm{A}}\,(\epsilon_0,v_1) - b\,\underline{\mathrm{N}}_0^2\right]\right\}^{-1} \times \langle\langle \mathbf{c}_2(t,t;v_1,v_2)\rangle\rangle . \tag{B8}$$

The intensity-correlation spectrum for a phase-diffusing field is obtained by combining components of Eq. (B8) to form $S_{\mathrm{out,out}}(\nu)$ [Eq. (19)].

[1] P. Zoller, Phys. Rev. A **20**, 2420 (1979).
[2] P. Zoller, G. Alber, and R. Salvador, Phys. Rev. A **24**, 398 (1981).
[3] H. Ritsch, P. Zoller, and J. Cooper, Phys. Rev. A **41**, 2653 (1990).
[4] Th. Haslwanter, H. Ritsch, J. Cooper, and P. Zoller, Phys. Rev. A **38**, 5652 (1988).
[5] R. Walser, H. Ritsch, P. Zoller, and J. Cooper, Phys. Rev. A **45**, 468 (1992).
[6] M. H. Anderson, R. D. Jones, J. Cooper, S. J. Smith, D. S. Elliott, H. Ritsch, and P. Zoller, Phys. Rev. Lett. **64**, 1346 (1990).
[7] M. H. Anderson, R. D. Jones, J. Cooper, S. J. Smith, D. S. Elliott, H. Ritsch, and P. Zoller, Phys. Rev. A **42**, 6690 (1990).
[8] T. Yabuzaki, T. Mitsui, and U. Tanaka, Phys. Rev. Lett. **67**, 2453 (1991).
[9] D. H. McIntyre, C. E. Fairchild, J. Cooper, and R. Walser, Opt. Lett. **18**, 1816 (1993).
[10] A. Icsevgi and W. E. Lamb, Jr., Phys. Rev. **185**, 517 (1969).
[11] J. H. Shirley, Phys. Rev. A **8**, 347 (1973).
[12] M. Lax, Phys. Rev. **145**, 110 (1966).
[13] W. H. Louisell, *Quantum Statistical Properties of Radiation* (Wiley-Interscience, New York, 1990).
[14] S. Machida, Y. Yamamoto, and Y. Itaya, Phys. Rev. Lett. **58**, 1000 (1987).
[15] C. Xie, G. Klimeck, and D. S. Elliott, Phys. Rev. A **41**, 6376 (1990).
[16] C. W. Gardiner, *Handbook of Stochastic Methods* (Springer, Berlin, 1990).
[17] B. R. Mollow, Phys. Rev. A **12**, 1919 (1975).